

Article

Selenium/Chitosan-Folic Acid Metal Complex Ameliorates Hepatic Damage and Oxidative Injury in Male Rats Exposed to Sodium Fluoride

Samy M. El-Megharbel¹, Fawziah A. Al-Salmi², Moamen S. Refat¹ and Reham Z. Hamza^{2,*} 

¹ Chemistry Department, College of Sciences, Taif University, P.O. Box 11099, Taif 21944, Saudi Arabia; s.megherbel@tu.edu.sa (S.M.E.-M.); Moamen@tu.edu.sa (M.S.R.)

² Biology Department, College of Sciences, Taif University, P.O. Box 11099, Taif 21944, Saudi Arabia; f.alsalmi@tu.edu.sa

* Correspondence: dr_reham_z@yahoo.com or Reham.z@tu.edu.sa

Abstract: Continuous exposure to sodium fluoride (NaF) imbalances the oxidative status in the body. The current study investigated the effect of the selenium/chitosan-folic (Se/chitosan-folic acid) novel metal complex on oxidative injury and tissue damage in the hepatic tissues of male rats exposed to (NaF). Male rats received NaF (10.3 mg/kg) and Se/chitosan-folic acid (0.5 mg/Kg) orally for successive 30 days. Male rats exposed to NaF showed multi-histopathological alterations in the hepatic tissues including degenerative changes. NaF exposure elevated hepatic oxidative stress markers, lipid peroxidation, and lowered the antioxidant defense enzymes. Se/chitosan-folic acid novel complex supplementation significantly prevented hepatic injury, suppressed reactive oxygen species (ROS) generation and lipid peroxidation, and enhanced the antioxidant defense enzymes. In addition, Se/chitosan-folic acid supplementation improved the hepatic tissues of NaF-exposed male rats. In conclusion, the Se/chitosan-folic acid novel metal complex protects against NaF-induced oxidative injury and tissue injury in the hepatic tissues of male rats. The Se/chitosan-folic acid novel metal complex upregulated the hepatic tissues and enhanced the antioxidant defense enzymes in male rats.

Keywords: drug metal complexes; sodium fluoride (NaF); chitosan; oxidative stress; folic acid; hepatic enzymes



Citation: El-Megharbel, S.M.; Al-Salmi, F.A.; Refat, M.S.; Hamza, R.Z. Selenium/Chitosan-Folic Acid Metal Complex Ameliorates Hepatic Damage and Oxidative Injury in Male Rats Exposed to Sodium Fluoride. *Crystals* **2021**, *11*, 1354. <https://doi.org/10.3390/cryst11111354>

Academic Editors: Assem Barakat and Alexander S. Novikov

Received: 20 October 2021

Accepted: 4 November 2021

Published: 8 November 2021

Publisher's Note: MDPI stays neutral with regard to jurisdictional claims in published maps and institutional affiliations.



Copyright: © 2021 by the authors. Licensee MDPI, Basel, Switzerland. This article is an open access article distributed under the terms and conditions of the Creative Commons Attribution (CC BY) license (<https://creativecommons.org/licenses/by/4.0/>).

1. Introduction

Sodium fluoride (NaF) is the most widely used chemical compound in fluorinated drinking water, toothpastes, and mouthwashes [1]. It was reported that about 21 countries have severe problems with endemic fluorosis, as the main pathway of fluoride exposure is contaminated groundwater. Sodium fluoride is widely distributed in the environment and extensively used. NaF is naturally present in many water sources as NaF is released from the runoff of F-containing rocks, leading NaF to leach into the groundwater [2].

In large areas, drinking water is artificially fluoridated, so water consumption is considered as the largest contributor to daily NaF intake. Additionally, NaF is involved in many insecticide formulations, foodstuffs, drugs, and industrial vapors emitted by using fluoride-containing compounds [3]. NaF is known to cross the cell membranes and to enter many soft tissues [4]. Fluorosis is a progressive and slow process causing metabolic and structural damages affecting many body tissues, particularly hepatic tissues [2].

NaF crosses the cellular membranes in a rapid way [5]. It is distributed in the hepatic tissues, cardiac muscle, and red blood cells [6,7]. The high toxicity of NaF arises from its high reactive ion. A study indicated that NaF inhibited the protein synthesis, and this is the main mechanism responsible for dental fluorosis in male mice given water containing high doses of NaF for 30 successive days [8].

Oxidative stress was found to be produced by NaF in the hepatic tissues of rabbits [8]. Oxidative damage and reduced antioxidant defense enzymes play a key vital role in the induction of the toxic effects of NaF [9]. Continuous exposure of NaF resulted in elevated lipid peroxidation and decreased the cellular defenses in different organs [10]. In the same context, therefore, resistance to oxidative injury might be an effective and potent way in preventing the pro-oxidant and other deleterious effects of NaF continuous exposure.

Selenium (Se) is an important trace element that is essentially required for humans, and plays a vital role in aspects of public health, essentially as an antioxidant agent; it plays a vital role in protecting tissues from oxidative damage [11]. Se deficiency might unbalance the antioxidant enzymes in the body and eventually elevate the risks associated with oxidation processes. It is necessary to meet the daily required supplementation of Se. Se deficiency is essentially associated with hepatic injury. Oxidative stress is an essential aspect of many hepatic diseases induced by toxins, autoimmune diseases, and so on. Many recent studies have indicated that hepatic damage can be elicited by Se deficiency, and that hepatic damage can be recovered by Se supplementation [12].

The antioxidant potential of Se plays an essential part in the hepatoprotective role. Recently, selenium nanoparticles have attracted high attention due to their excellent biological activities. Selenium nanoparticles exhibit great potential for use in nutritional supplementation [13]. The hepatoprotective effect of selenium nanoparticles seems to be promising due to their high antioxidant capacities [14].

Chitosan (CH), the only natural positively charged polysaccharide, has recently been extensively used in drug delivery systems. Chitosan is mainly composed of D-glucosamine and is obtained by the deacetylation of chitin. The biocompatibility and lower toxicity of chitosan have led to its use in several biomedical applications, and it also has high antioxidant and anti-inflammatory effects [15]. Additionally, there is a chemical modification and formula of chitosan for the enhancement of its chemical properties such as high solubility and bioactivities, for example, the conjugation of naturally active molecules onto chitosan leads to enhancement in the bioactivities and its solubility. Chitosan embedded with selenium nanoparticles proved their hepatoprotective effect [16].

Folic acid (FA), which is known as (vitamin B9), is an essential vitamin for DNA synthesis and cellular division. Additionally, it possesses antioxidant activities; it can scavenge the excessive free radicals, thus preventing cellular injury [17]. FA interacts with No-synthase and declines the formation of O_2^- . It has been shown that FA has a hepatoprotective effect and a high antioxidant effect [18]. To our knowledge, the hepatoprotective effects of the novel complex of (selenium-chitosan/folic acid) Se/chitosan-folic acid against NaF-induced hepatotoxicity have not been determined yet. Thus, the present study was conducted to examine the protective effects of the Se/chitosan-folic acid novel complex against NaF-induced hepatotoxicity and the possible mechanisms underlying these effects.

In this study, selenium-stabilized chitosan and folic acid (Se-CH/FO) were prepared. In addition, the hepatoprotective effect of Se/chitosan-folic acid against hepatotoxicity induced by sodium fluoride was studied. Therefore, this study investigated the ameliorative effects of the Se/chitosan-folic acid novel complex against NaF-induced oxidative injury and hepatotoxicity.

2. Materials and Methods

2.1. Chemicals

The available chemicals were used commercially without further purification and purchased from Sigma-Aldrich (Burlington, MA, USA). Chitosan had a low molecular weight (60–190 kDa), with a degree of deacetylation of 80–85%. Selenium tetrachloride Se^{+4} had a purity $\geq 98\%$. $K_2S_2O_8$ (potassium persulfate) had a purity of 99.9%. C_2H_5OH (ethanol) and glacial acetic acid were also used in the experiment. IR spectral data for the prepared complex were determined using a Bruker infrared spectrophotometer (Milton, Ontario, Canada) at a range of 400–4000 cm^{-1} . The conductance measurement was conducted with a concentration of 10^{-3} M for the synthesized complex using di-methyl

sulfoxide DMSO (Sigma Aldrich, St. Louis, MO, USA). The electronic absorption spectra were recorded in the DMSO solvent within the 800–200 nm range using a UV2 Unicam UV/Vis Spectrophotometer (Mettler-Toledo, Columbus, OH, USA) fitted with a quartz cell with a 1.0 cm path length. The surface morphologies for the particles of the complex were visualized using Quanta FEG 250 scanning (JEOL SEM-6400, Jeol, Tokyo, Japan) and transmission (JEOL JEM-3300, Tokyo, Japan) electron microscopes generated at a 20 kV accelerating voltage. The shapes and sizes of these particles were visualized using JEOL JEM-1200 EX II (Tokyo, Japan) and JEOL 100 s microscopy (Tokyo, Japan), respectively. The Zeta potential distributions of complex were performed using 1% acetic acid.

2.2. Synthesis of Se/Chitosan

The purification of chitosan was carried out [19] using 1% acetic acid to dissolve the chitosan. The solution was subjected to filtration to remove any impurities. Next, NaOH (2 M) was added to the chitosan solution and stirred for 1 h. Then, filtration was performed, and the solution was washed using distilled water and adjusted to a pH level of 7. The sample was frozen for 72 h. Using thiourea, purified chitosan was prepared for Se/chitosan, which acted as a sulfur source for the preparation of selenium sulfide nanoparticles [20]. In addition, during preparation, about 3.0 mmol of high purified chitosan was added to the distilled water (150 mL). After incorporation into the chitosan solution, a selenium salt solution (0.8 mmol in 40 mL distilled water) was added drop-wise. Additionally, the solution was subjected to stirring for 30 min to ensure homogeneity. After condensing for 8 h, the thiourea solution (0.09 mmol in distilled water 100 mL) was added drop-wise. Then, the mixture was cooled for 4 h. Ethanol (C₂H₅OH) was added to wash for the sample before drying for 72 h at 70 °C.

2.3. Preparation of Se/Chitosan-Folic Acid

After drying the chitosan-selenium sulfide, the prepared sample was dissolved by using 100 mL 1% acetic acid. Then, the solution was transferred into 5.43 mmol folic acid in a flask with continuous stirring for 5 min. The sample was then immersed in a water bath until reaching 70 °C, and potassium persulfate (3.7 mmol) was added to accelerate the degradation of chitosan and the participation of folic acid into the mixture [21]. Then, the sample was subjected to filtration. Finally, the resulting sample was dried (Figure 1).

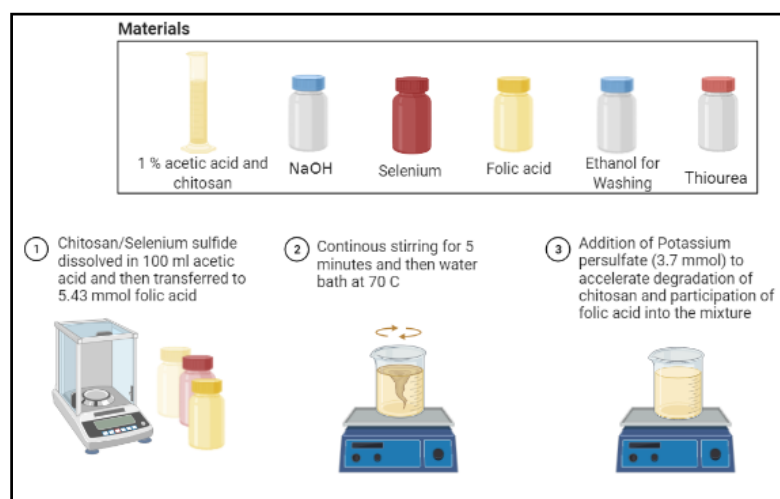


Figure 1. Synthesis of selenium/chitosan-folic acid complex.

2.4. Experimental Animals and Treatments

A total of 40 two-month-old male Wistar Albino rats weighing (150–180 g) were used in this study (10 rats/each group). The male rats were kept under high standard conditions of temperature and humidity under a regular 12 h light/dark cycle and supplied water and

food *ad libitum*, and all the experimental animals completed the experiment without any mortality. The experiment was undertaken under the approval of the ethical committee of the Deanship of Scientific Research under approval number 39-31-0043. The rats were divided into groups as follows.

Group I (control group) received 1 mL gum acacia emulsion (1%) orally as the vehicle; Group II (sodium fluoride NaF) received an oral dose of 10.3 mg/Kg [1]; Group III (selenium-chitosan/folic acid complex) received 0.5 mg/kg dissolved in vehicle orally as we determined 1/20 of LD50 of the complex at dose 0.5 mg/Kg; and Group IV (sodium fluoride NaF + Se/chitosan-folic acid complex) received sodium fluoride NaF first, followed by the Se/chitosan-folic acid complex after 30 min dissolved in the vehicle by oral gavage. All groups were treated for a successive 30 days.

Blood samples were collected from the eye plexus, which is more convenient, and pure blood with excessive bleeding, and serum was prepared by centrifugation at 5000 rpm for 20 min for the assay of alanine and aspartate aminotransferases (ALT and AST). The male rats were dissected after light anesthesia with ketamine/xylazine, liver tissues were collected, and samples were fixed in 10% neutral buffered formalin for histopathological examination. The other samples were homogenized (10% *w/v*) in cold phosphate-buffered saline (PBS) and centrifuged. Then, the supernatant was collected, stored at $-80\text{ }^{\circ}\text{C}$, and used for the further investigation of the antioxidant enzymes.

2.5. Biochemical Assays

ALT and AST enzymes were determined in the serum using assay kits (Spinreact, Barcelona, Spain), following the manufacturer's instructions. Malondialdehyde (MDA), a marker of LPO, was assayed in the liver tissues according to the methods described by the authors of [22]. Reduced glutathione (GSH) [23], superoxide dismutase (SOD) [24], and catalase (CAT) [24] were determined in the homogenates of the liver tissues.

2.6. Histopathological Study

Liver tissues were fixed in 10% neutral buffered formalin for about 24 h and were dehydrated, cleared in xylene, and embedded in paraffin wax. Then, 5 μm sections were cut using a microtome, processed for hematoxylin and eosin (H&E) staining [25], and examined using a light microscope.

2.7. Statistical Analysis

The results are presented as mean \pm standard error of the mean (SEM). Multiple comparisons were tested using one-way ANOVA followed by post hoc analysis (San Diego, CA, USA). *p*-values below 0.05 were considered as significant.

3. Results

3.1. Microanalytical and Molar Conductance Data

Se/chitosan-folic acid has a high stability at room temperature, a low solubility in most solvents, and a high solubility in Di-methylformamide DMF and DMSO with gentle heating. The conductance measurement of Se/chitosan-folic acid complex was 21 $\mu\text{s}/\text{cm}$. The electrolytic measurement of the Se(IV) complex showed a ratio of 1:1:1 (folic acid:chitosan:selenium). The low conductivity measurement value of 10^{-3} M solution in the DMSO was the non-electrolyte.

3.2. FTIR Studies

The IR spectra for the derivatives of chitosan (Figure 2) demonstrated peaks specific to functional groups. For chitosan, the peak at 3288 cm^{-1} represented the stretching vibrations of the hydroxyl and amino groups. The stretching C–H vibrations of chitosan at 2916 cm^{-1} and 2880 cm^{-1} have been described in the literature [26]. The C=O stretching vibration at 1630 cm^{-1} was attributed to the NH–CO amide I group. In addition, the amide group II appeared at 1592 cm^{-1} , with bending vibrations attributed to the N–H amide group [27].

For chitosan, peaks in the ring structure at 1416 cm^{-1} and 1330 cm^{-1} represent O–H and C–H vibrations, respectively. The carbon–nitrogen vibrations and bending motions of the amide N–H appeared at 1280 cm^{-1} . For chitosan, the peaks between 1149 cm^{-1} and 800 cm^{-1} corresponded to the C–O stretching vibrations [27]. After the reaction of chitosan with selenium, a shift was observed for the stretching amino group at 3268 cm^{-1} , the stretching C–H group at 2890 cm^{-1} , and the amide I and II peaks at 1620 cm^{-1} and 1575 cm^{-1} , respectively.

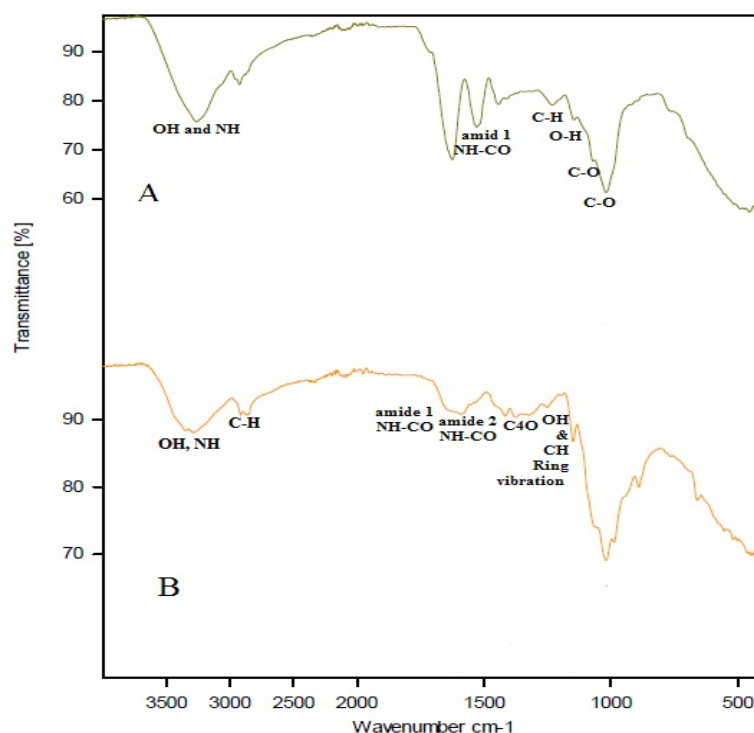


Figure 2. FTIR of **A**—Se/chitosan-folic acid. The IR for Se/chitosan-folic acid showed peaks attributed to NH_2 and OH stretching between 3265 cm^{-1} and 2928 cm^{-1} (broad band). In addition, a shift was observed at 1529 cm^{-1} for amide I peak 1 in Se/chitosan-folic acid and stretching vibrations of C–O at 1019 cm^{-1} and 892 cm^{-1} (sharp band), corresponding to changes occurring after complexation with folic acid. Due to the O–H ring, there was a peak at 1400 cm^{-1} (weak band), which disappeared in the Se/chitosan-folic acid spectrum, and a new other peak appeared at 1398 cm^{-1} (weak band). **B**—chitosan. The IR for chitosan showed a peak at 3290 cm^{-1} (broad band) referring to the vibrational stretching motions of the OH and NH_2 groups. The peaks at 2920 cm^{-1} and 2885 cm^{-1} (very weak band) were due to the vibration of C–H, and that at 1635 cm^{-1} was due to the amide I group NH–CO (broad shoulder band). The NH–CO amide group II appeared at 1595 cm^{-1} (broad shoulder band). The peaks at 1420 cm^{-1} and 1335 cm^{-1} refer to the OH and C–H vibrations, respectively. Therefore, there is a chelation occurring between selenium, folic acid, and chitosan.

These shifts in the positions of the peaks can be attributed to the complexation of selenium and chitosan [28,29]. The IR for Se/chitosan-folic acid showed peaks attributed to amino and hydroxyl stretching between 3265 cm^{-1} and 2928 cm^{-1} . In addition, a shift at 1529 cm^{-1} for amide I peak 1 was observed in Se/chitosan-folic acid when compared to the chitosan and Se/chitosan complex, along with a C–H vibration of CH_3 at 1413 cm^{-1} , C–H ring vibrations at 1300 cm^{-1} , and stretching vibrations of C–O at 1019 cm^{-1} and 892 cm^{-1} , corresponding to changes occurring after complexation with folic acid. Due to the hydroxyl vibrations at the O–H ring, there was a peak at 1400 cm^{-1} , which disappeared in the Se/chitosan-folic acid spectrum due to the peak at 1398 cm^{-1} from the C–H vibration. The C–H vibration peak led to masking, which created shifts at 1361 cm^{-1} and 1376 cm^{-1} .

Based on the above-mentioned data, we can conclude that the incorporation of folic acid and chitosan occurred.

3.3. UV–Visible Measurements

According to previous studies, chitosan does not show absorbance due to its lack of double bond conjugations (Figure 3) [27]. In Se/chitosan, a peak appeared at 230 nm. This peak demonstrates that chitosan was no longer in the wavelength compared to the pure chitosan at 208 nm, confirming the complexation between Se and chitosan. In addition, from 2750 nm to 340 nm, a broad peak appeared for Se/chitosan due to the nanocrystal Se, which had a lower wavelength compared with the bulk Se (345 nm) [27]. On the other hand, increasing wavelengths were observed for Se/chitosan-folic acid at 228 nm. In addition, Se/chitosan-folic acid demonstrated an absorption peak between 265 nm and 325 nm, confirming the presence of folic acid [30]. Pure folic acid has shown absorption peaks at wavelengths of 256 nm, 284 nm, and 366 nm [31]. The main differences observed between Se/chitosan-folic acid and the solutions of folic acid confirmed the complexation of Se/chitosan and folic acid.

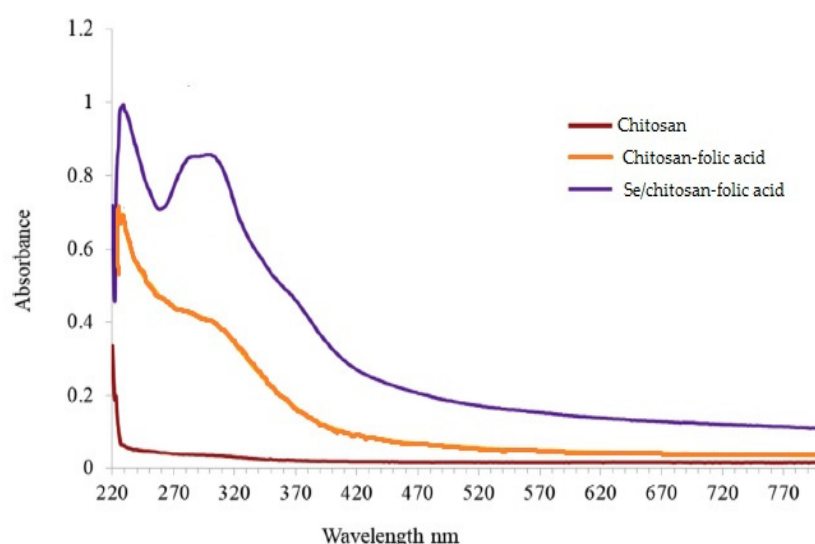


Figure 3. UV–Vis absorbance spectra of chitosan, chitosan-folic acid, and Se/chitosan-folic acid.

3.4. SEM Studies

In the SEM images, Se/chitosan-folic acid (Figure 4) and pure chitosan were tuft-like and pored, while Se/chitosan appeared coarse with a disparate surface. The surface morphology of Se/chitosan-folic acid is in agreement with the previously reported data [32]. After folic acid complexation, the sample's surface structure appeared spherule-like, confirming the formation of the Se/chitosan-folic acid complex.

3.5. Transmittance Electron Microscopy (TEM)

The TEM image of the [Se(folic)(chitosan)] complex nanoparticles resulting from the reaction of SeCl_4 salt with folic acid and chitosan in an alkaline medium is shown in Figure 5. After the complexation, particle size was found to be in the approximate ranges between 8, 12, and 50 nm with spherical black spots.

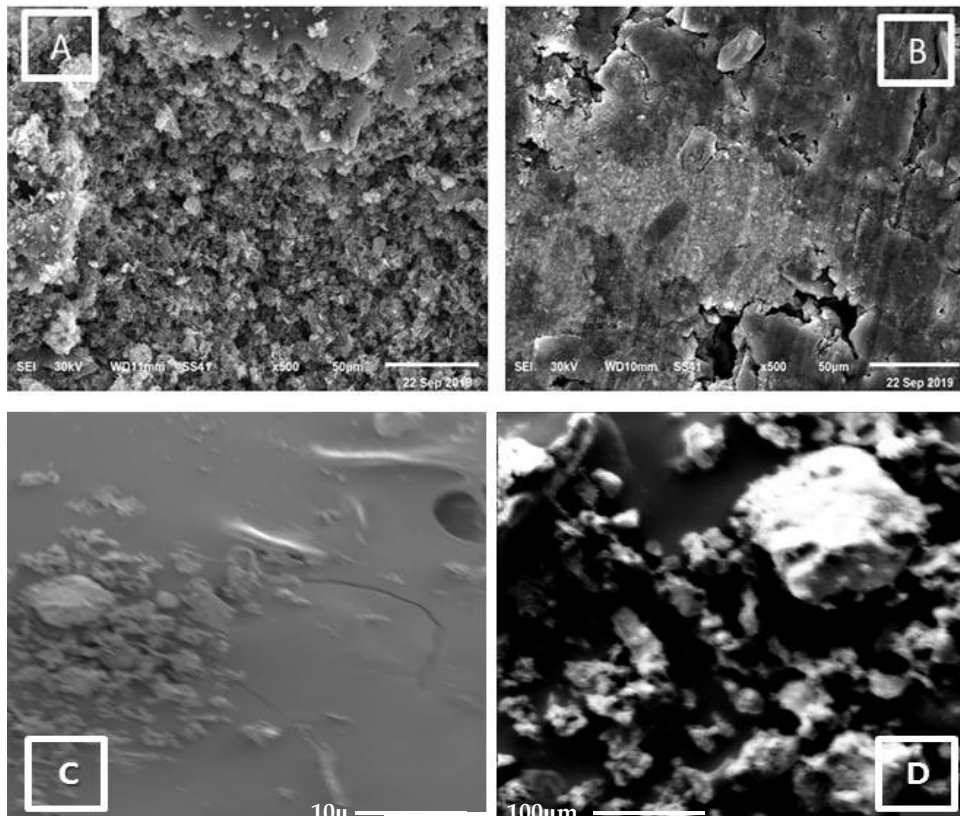


Figure 4. (A–D). SEM image of the [Se(Folic)(Chitosan)] complex. (A) Small attached amorphous granules; (B) Coarse surface with a disparate; (C) Tuft-like and aggregated pored structure (D); and straight and pointed particles.

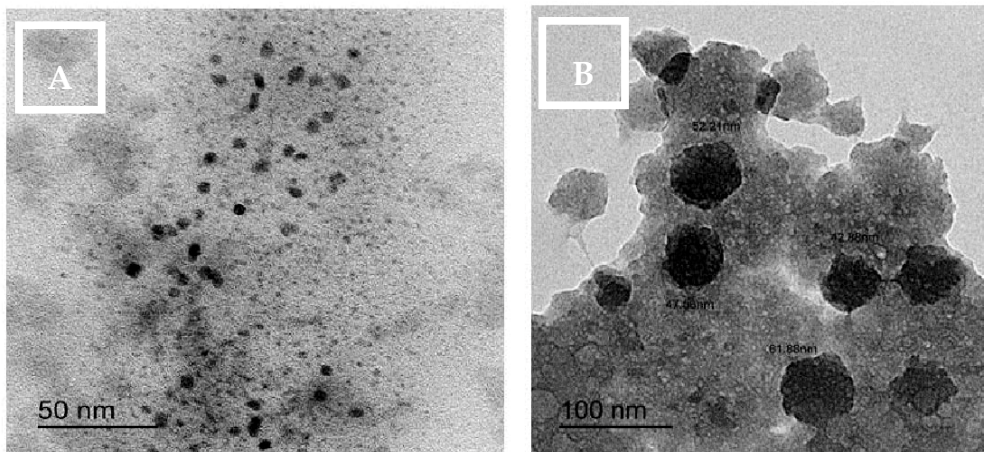


Figure 5. TEM image of [Se(folic)(chitosan)] complex. (A) Small black spots. (B) Black spots dispersed in gelatinous media.

3.6. Size and Zeta Potential

The average size of the (Se/chitosan-folic acid sample in 1% acetic acid was found to be about 42.88–61.88 nm (Figure 6), and the polydispersity index (PDI) was about 0.29. The PDI value below 0.300 indicates that the particle size had a narrow distribution. The Zeta potential measurements were carried out for chitosan and Se/chitosan-folic acid samples dissolved in 1% acetic acid. From the analyzed samples, pure chitosan had a high positive Zeta potential value of 60.06 ± 0.55 mV. This high +ve value is expected for the chitosan, as its pKa is w6.5, making it positively charged under acidic conditions. In addition, significantly higher positive Zeta potential values have been reported for chitosan under

acidic conditions [27]. The Se/chitosan-folic acid sample had a ZP (zeta potential) value of 58.63 ± 0.93 mV, which is close to the values observed before for similar samples [27]. Then, the ZP of Se/chitosan-folic acid was measured to be 49.57 ± 1.62 mV. However, this high +ve Zeta potential indicates that the nanoparticles were stable under the given conditions and held great potential for the uptake through the negatively charged cell membrane.

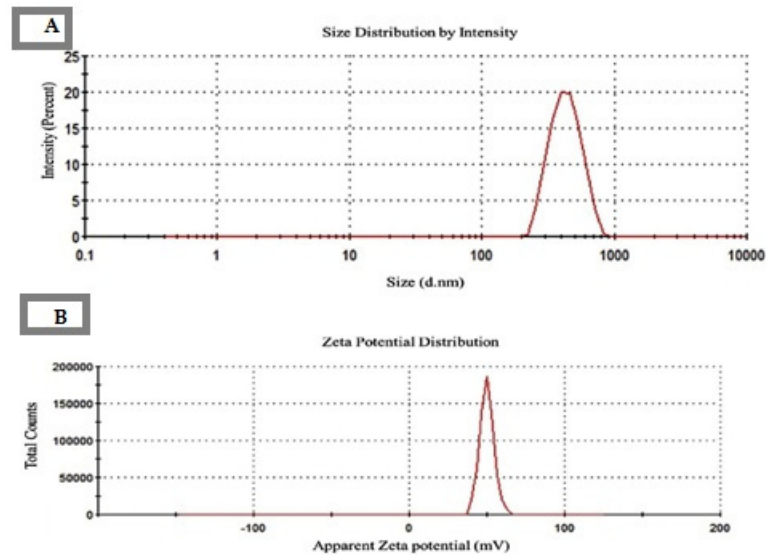


Figure 6. Se/chitosan-folic acid. (A) Average size and polydispersity index, and (B) Zeta potential range.

3.7. Selenium-Chitosan/Folic Acid Ameliorates Hepatic Damage

Successive exposure to NaF for a successive 30 days significantly increased the serum activities of ALT (Figure 7A) and serum AST (Figure 7B) ($p < 0.001$) in male rats. In contrast, oral supplementation of the Se/chitosan-folic acid novel complex ameliorated the serum ALT and AST in NaF-induced hepatotoxicity in male rats.

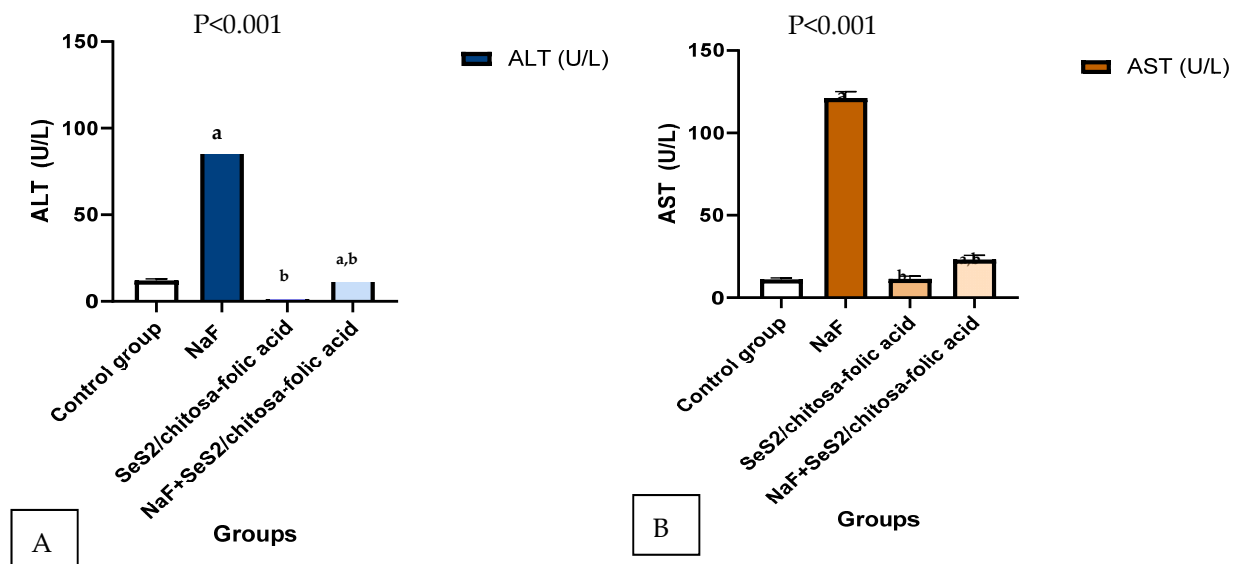


Figure 7. Se/chitosan-folic acid novel complex ameliorated serum ALT and AST in NaF-exposed male rats. Data are mean \pm SEM, $n = 10$. (A) Alanine aminotransferase; (B) Aspartate aminotransferase. Where (a) is significant to the control group, (b) is significant to the NaF treated group.

The histological examination supports the hepatoprotective effects of the Se/chitosan-folic acid novel complex in male rats. Whereas the control group (Figure 8A) and Se/chitosan-

folic acid novel complex-supplemented group (Figure 8C) exhibited normal hepatic structures of the hepatic lobules, hepatocytes, and sinusoids, the NaF-exposed male rats showed congestion in the central vein and high degenerative alterations (Figure 8B). Treatment with the Se/chitosan-folic acid novel complex markedly prevented NaF-induced liver histological alterations in the male rats (Figure 8D).

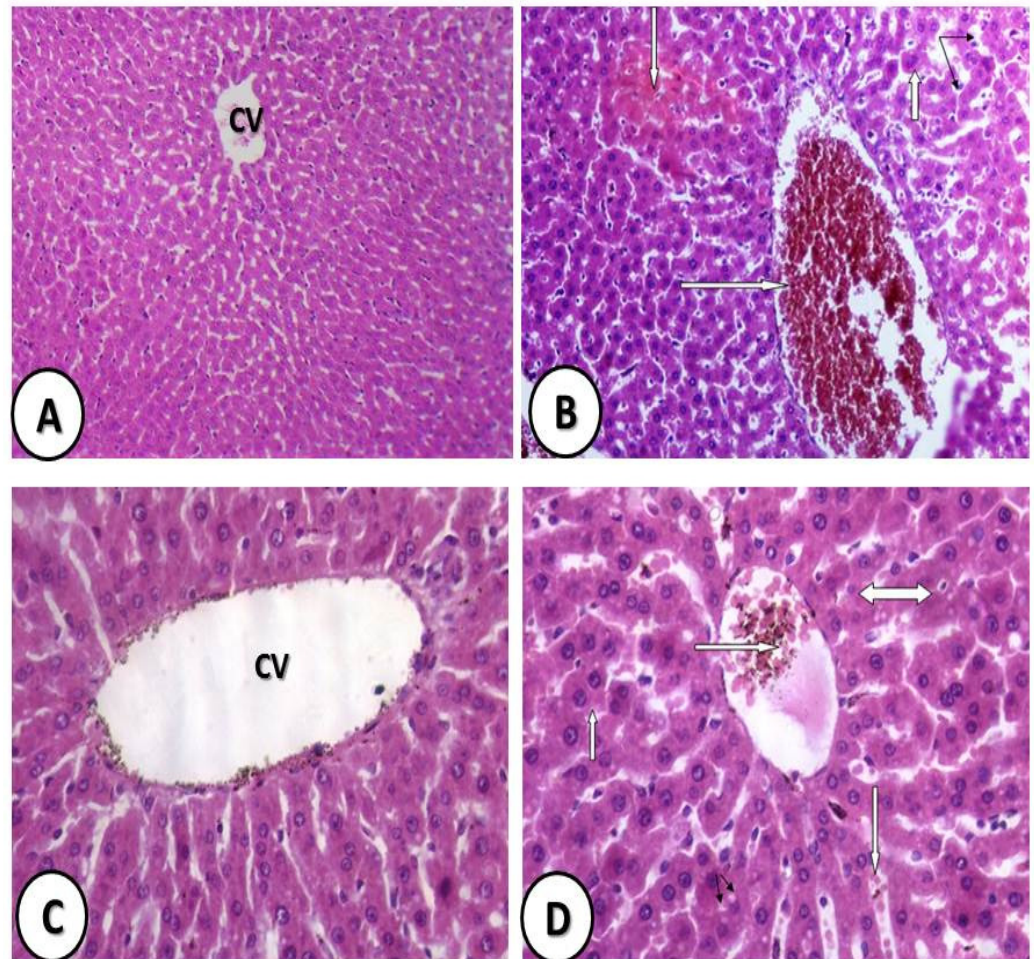


Figure 8. Photomicrographs of H&E-stained sections in the liver of the (A) control group showing normal hepatic cells and (B) sodium fluoride (NaF)-treated male rats showing a photomicrograph of the cross section of the experimental rat liver after administration of toxic substances showing severe toxicity in the form of hypertrophy of hepatocytes with the appearance of binucleated hepatocytes and increased eosinophilia, granular cytoplasm, and vesicular nuclei (↓); the central vein is dilated and filled with hemorrhage and necrotic tissue (⇨); focal necrosis in some hepatocytes with increased eosinophilia and nuclear disappearance; and the accumulation of a few mononuclear inflammatory cells in blood sinusoids (↘). (C) Se/chitosan-folic acid-treated male rats showing normal hepatic structure with dilated central vein. (D) NaF + Se/chitosan-folic acid-treated group showing photomicrograph of the cross section of the experimental rat liver after the administration of toxic substances showing mild toxicity in the form of hypertrophy of hepatocytes with granular eosinophilic cytoplasm and vesicular nuclei and the appearance of some binucleated cells (↑↑), with mild congested central vein containing mild brown particles of bilirubin, indicating biliary tract obstruction, ballooning degeneration in some hepatocytes, and few dilated congested blood sinusoids as well as focal and single hepatocyte necrosis (⇨⇨). Scale bar = 50 μm.

3.8. The Se/Chitosan-Folic Acid Novel Complex Attenuates Oxidative Stress in the Livers of Male Rats Exposed to Sodium Fluoride

In contrast, male rats exposed to NaF exhibited significant decreases in hepatic GSH content (Figure 9) and SOD and CAT activity when compared with the control group. Administration of the Se/chitosan-folic acid novel complex elevated GSH and antioxidant enzymes in the liver tissues of NaF-exposed male rats.

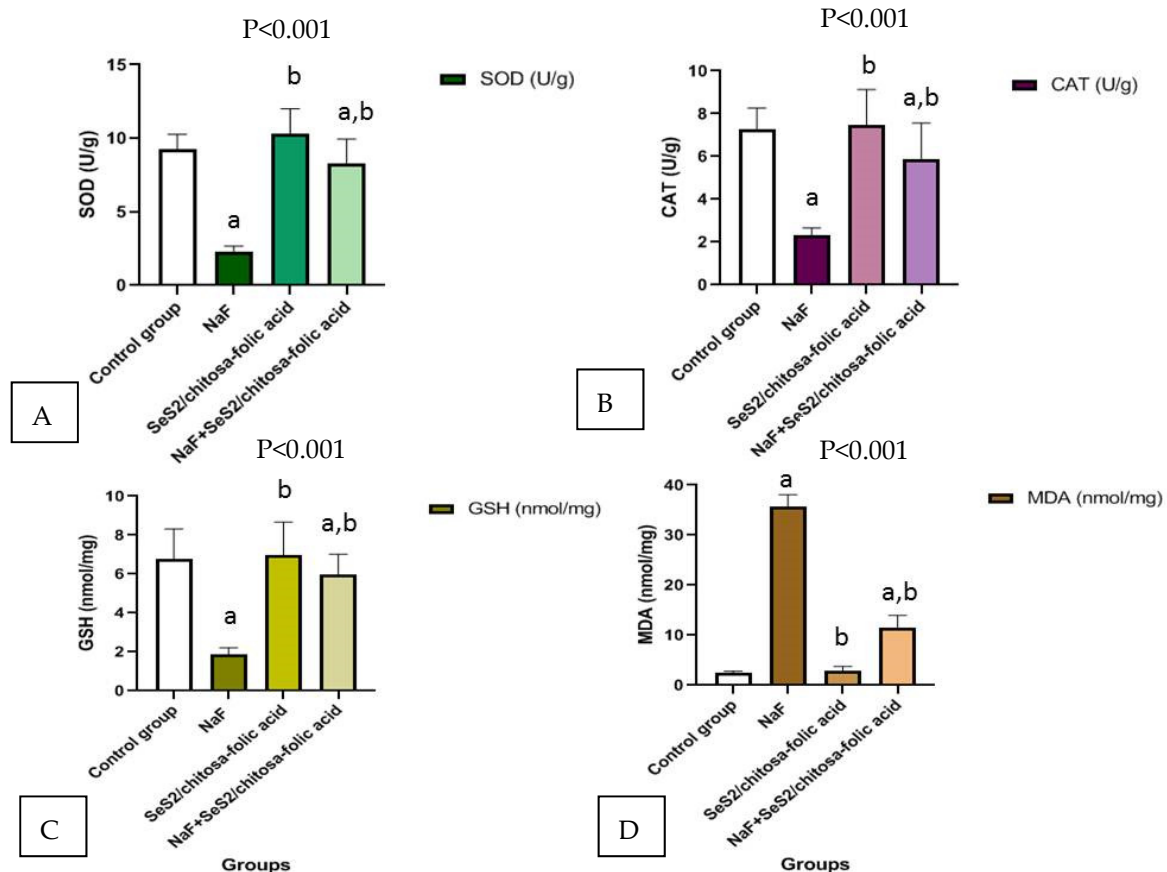


Figure 9. Se/chitosan-folic acid novel complex decreased MDA, GSH, SOD, and CAT in the liver tissues of sodium fluoride NaF-exposed male rats. Data are mean \pm SEM, $n = 10$. (A) SOD enzyme; (B) CAT enzyme (C); GSH enzyme (D); MDA (marker of lipid peroxidation) Where (a) is significant to the control group, (b) is significant to the NaF treated group.

4. Discussion

ROS such as H_2O_2 , OH^- , and O_2^- play vital roles in the progression of chemical-induced intoxications and the induction of severe oxidative stress [33]. Under severe oxidative stress conditions, ROS directly participates in the pathogenesis of many diseases [34]. The human body is well equipped with many antioxidant enzymes such as superoxide dismutase (SOD), catalase (CAT), and non-enzymatic antioxidants including reduced glutathione (GRx) [35]. The generation of high levels of free radicals can result in severe oxidative damage to large molecules, tissues, and body organs [36].

Antioxidants can scavenge excessive free radicals. The biological and pharmacological activities of folic acid, selenium, and chitosan have not been reported until now. Thus, the antioxidant activity of these antioxidants and their beneficial effects in the treatment of severe oxidative diseases have received significant attention [37]. To date, no scientific report has been published describing the protective role of the combined complex of folic acid, selenium, and chitosan against sodium fluoride-induced hepatotoxicity and oxidative stress in liver tissues. The present study demonstrated that intoxication with sodium fluoride induced hepatotoxicity and severe oxidative stress, which could be mitigated by the administration of Se/chitosan-folic acid.

Lipid peroxidation is the essential parameter of oxidative stress, and malondialdehyde (MDA) is considered as the index of lipid peroxidation markers. MDA is the breakdown product of the chain reaction of polyunsaturated fatty acid oxidation and serves as a marker of lipid peroxidation in tissues [38]. In this study, intoxication with sodium fluoride increased the MDA levels and, therefore, the extent of lipid peroxidation in the hepatic tissues of the NaF-intoxicated animals.

Increased lipid peroxidation is improved due to the release of iron, which occurs due to Fenton-type reactions [39]. Glutathione plays an important role in antioxidant defense against ROS [40]. During oxidative stress, glutathione is oxidized to form disulfide links known as oxidized glutathione. In this study, a significant change in the glutathione levels was observed in the NaF-intoxicated animals.

We have previously illustrated how chitosan and chitosan nanoparticles induced hepatoprotective effects and elicited antioxidant capacities and improved other biochemical indicators [16]; we have also highlighted the potential usefulness of using either selenium or selenium nanoparticles in alleviating the hepatic damage and injury induced by several pollutants and xenobiotics [12–14]. Therefore, we have great empirical confirmation on the vitality and activity of each component alone, and we wanted to shed light on the importance of using the novel complex of chitosan, selenium, and folic acid in improving hepatic functions and alleviating oxidative stress induced by NaF as a first knowledge in the literature on this formula; we provided additional evidence on the novel complex's high abilities in improving hepatic tissue structure after confirming its chemical structure by FTIR, SEM, and TEM examination.

Administration of the Se/chitosan-folic acid novel complex after NaF intoxication mitigated abnormalities in the intracellular antioxidant levels with their metabolites. NaF intoxication decreased the SOD activity in the hepatic tissues due to the accumulation of extra O_2^- in the hepatic tissues. In addition, the decreased CAT activity in NaF-intoxicated rat livers may be elucidated by the inadequate supply of nicotinamide adenine dinucleotide phosphate (NADP) required for catalase activation from its inactivated form [41].

The serum biochemistry also revealed that the enzymatic activities of AST and ALT, which play an important role in hepatic diseases [42], were elevated by the administration of NaF, whereas these enzymatic activities were decreased by co-administration with the Se/chitosan-folic acid novel complex.

Several studies have demonstrated the potent hepatoprotective effects of natural antioxidants such as chitosan through their high capacity to scavenge the reactive oxygen species [43]. The mechanisms of the Se/chitosan-folic acid novel complex, with respect to its antioxidant properties, include its free radical scavenging activity as well as its lipoxygenase and cyclooxygenase inhibition and cellular membrane-stabilizing activity [44]. The Se/chitosan-folic acid novel complex has also been shown to inhibit oxidative enzymes [45].

The current study is in agreement with parallel results to those found by Tzankova et al. [46]. In their study, the researchers confirmed that pretreatment with quercetin encapsulated in chitosan–alginate nanoparticles, which is similar in formula to our novel complex, had effective protection against paracetamol-induced hepatotoxicity in male Wistar rats. The peroxidation of membrane lipids has been recognized as an important mechanism of oxygen/free radical toxicity [47]. Therefore, lipid peroxidation is a sensitive marker of ROS-mediated cell damage. Our data showed that treatment with NaF elevated the MDA levels in the hepatic tissues, implying enhanced peroxidation. Oral pretreatment with the encapsulated Se/chitosan-folic acid novel complex significantly decreased the MDA levels compared with the NaF treatment group, suggesting a protection against drug-induced lipid peroxidation.

These results were consistent with those of other studies, which have noted the beneficial effects of folic acid [48], selenium [49], and chitosan [16] on the cellular membrane lipids, the improvement of hepatic functions, and the alleviation of oxidative stress [50].

The current study revealed an improvement in the hepatic function parameters and antioxidant defense mechanism in the group treated with the Se/chitosan-folic acid novel

complex. These results are in complete agreement with a previous study [51,52] that demonstrated that concomitant treatment with folic acid, which is a vital part of the novel complex explored in this study, attenuated the Pb-induced hepatotoxicity and biochemical alterations. These effects were indicated by reductions in the portal and lobular inflammatory cell infiltration and the presence of hydropic degeneration, as confirmed in the current study.

5. Conclusions

The present study introduced new information on the hepatoprotective effects of the Se/chitosan-folic acid novel complex against NaF-induced hepatic injury. Se/chitosan-folic acid prevented histopathological alterations and suppressed ROS in the hepatic tissues of NaF-exposed male rats. In addition, Se/chitosan-folic acid upregulated the hepatic antioxidant defense system, thereby preventing NaF-induced severe oxidative stress. Therefore, Se/chitosan-folic acid may be considered as a potential candidate for attenuating NaF-induced liver alterations in male rats, pending further studies to explore the other mechanisms involved in the protective effects of this novel complex.

Author Contributions: Conceptualization, S.M.E.-M., M.S.R. and R.Z.H.; Methodology, S.M.E.-M., M.S.R., F.A.A.-S. and R.Z.H.; Validation, S.M.E.-M. and R.Z.H.; Formal analysis, S.M.E.-M., M.S.R., F.A.A.-S. and R.Z.H.; Investigation, S.M.E.-M. and R.Z.H.; Resources, S.M.E.-M., M.S.R., F.A.A.-S. and R.Z.H.; Data curation, M.S.R., S.M.E.-M. and R.Z.H.; Writing—original draft preparation, S.M.E.-M., F.A.A.-S., M.S.R. and R.Z.H.; Writing—review and editing, S.M.E.-M., M.S.R. and R.Z.H.; Visualization, S.M.E.-M., F.A.A.-S., M.S.R. and R.Z.H.; Supervision, S.M.E.-M., M.S.R. and R.Z.H.; Project administration, S.M.E.-M. and R.Z.H.; Funding acquisition, S.M.E.-M. and R.Z.H. All authors have read and agreed to the published version of the manuscript.

Funding: This research received no external funding.

Institutional Review Board Statement: The study was conducted according to the guidelines of the Declaration of Helsinki and approved by the Ethics Committee of King Saud University (KSA).

Informed Consent Statement: Not applicable.

Data Availability Statement: Data analyzed or generated during this study are included in this manuscript.

Acknowledgments: The authors acknowledge Taif University Researcher supporting project number (TURSP-2020/15), Taif University, Taif, Saudi Arabia.

Conflicts of Interest: The authors declare no conflict of interest.

References

1. Al-Harbi, M.S.; Hamza, R.Z.; Dwari, A.A. Sodium fluoride induced antioxidant defense impairment and impaired renal biomarkers and the ameliorative role of selenium and curcumin in male mice. *Asian Pac. J. Trop. Dis.* **2014**, *4* (Suppl. 2), S990–S997. [[CrossRef](#)]
2. Ismail, H.A.; Hamza, R.Z.; El-Shenawy, N.S. Potential protective effects of blackberry and quercetin on sodium fluoride induced impaired hepatorenal bi-omarkers, sex hormones and hematotoxicity in male rats. *J. Appl. Life Sci. Int.* **2014**, *1*, 1–16. [[CrossRef](#)]
3. National Research Council (NRC). *Fluoride in Drinking-Water: A Scientific Review of EPA's Standards*; National Academy of Sciences: Washington, DC, USA, 2006.
4. Aydin, G.; Çiçek, E.; Akdoğan, M.; Gökcalp, O. Histopathological and biochemical changes in lung tissues of rats following administration of fluoride over several generations. *J. Appl. Toxicol. Int. J.* **2003**, *23*, 437–446. [[CrossRef](#)] [[PubMed](#)]
5. Şireli, M.; Bülbül, A. The effect of acute fluoride poisoning on nitric oxide and methemoglobin formation in the guinea pig. *Turk. J. Vet. Anim. Sci.* **2004**, *28*, 591–595.
6. Akdoğan, M.; Bilgili, A.; Karaöz, E.; Gökçimen, A.; Eraslan, G.; Üstüner, E. The structural and biochemical changes of kidney tissue on fluorosis in rabbits. *Turk. J. Vet. Anim. Sci.* **2002**, *26*, 71–77.
7. Akdoğan, M.; Bilgili, A.; Karaöz, E.; Gökçimen, A.; Yarsan, E.; Eraslan, G. The structural and biochemical alterations in liver of rabbits, received flour with water for particular dose and period, FU. *J. Health Sci.* **2002**, *16*, 41–46.
8. DenBesten, P.; Li, W. Chronic fluoride toxicity: Dental fluorosis. *Fluoride Oral Environ.* **2011**, *22*, 81–96.
9. Hamza, R.Z.; Al-Harbi, M.S. Amelioration of paracetamol hepatotoxicity and oxidative stress on mice liver with silymarin and *Nigella sativa* extract supplements. *Asian Pac. J. Trop. Biomed.* **2015**, *5*, 521–531. [[CrossRef](#)]

10. Hamza, R.Z.; El-Shenawy, N.S.; Ismail, H.A.A. Protective effects of blackberry and quercetin on sodium fluoride-induced oxidative stress and histological changes in the hepatic, renal, testis and brain tissue of male rat. *J. Basic Clin. Physiol. Pharmacol.* **2015**, *26*, 237–251. [[CrossRef](#)]
11. Hamza, R.Z.; Diab, A.E.A.A. Testicular protective and antioxidant effects of selenium nanoparticles on Monosodium glutamate-induced testicular structure alterations in male mice. *Toxicol. Rep.* **2020**, *7*, 254–260. [[CrossRef](#)]
12. El-Shenawy, N.S.; AL-Harbi, M.S.; Hamza, R.Z. Effect of vitamin E and selenium separately and in combination on biochemical, immunological and histological changes induced by sodium azide in male mice. *Exp. Toxicol. Pathol.* **2015**, *67*, 65–76. [[CrossRef](#)]
13. Al-Harbi, M.S.; Hamza, R. Potential ameliorative effects of selenium and chromium supplementation against toxicity and oxidative stress in streptozotocin diabetic rats. *Int. J. Pharmacol.* **2016**, *12*, 483–495. [[CrossRef](#)]
14. Alharthi, W.A.; Hamza, R.Z.; Elmahdi, M.M.; Abuelzahab, H.S.; Saleh, H. Selenium and L-carnitine ameliorate reproductive toxicity induced by cadmium in male mice. *Biol. Trace Elem. Res.* **2020**, *197*, 619–627. [[CrossRef](#)]
15. Bai, K.; Hong, B.; He, J.; Huang, W. Antioxidant capacity and hepatoprotective role of chitosan-stabilized selenium nanoparticles in concanavalin a-induced liver injury in mice. *Nutrients* **2020**, *12*, 857. [[CrossRef](#)]
16. Al-Baqami, N.; Hamza, R. Synergistic antioxidant capacities of vanillin and chitosan nanoparticles against reactive oxygen species, hepatotoxicity, and genotoxicity induced by aging in male Wistar rats. *Hum. Exp. Toxicol.* **2021**, *40*, 183–202. [[CrossRef](#)]
17. Badary, D.M. Folic acid protects against lead acetate-induced hepatotoxicity by decreasing NF- κ B, IL-1 β production and lipid peroxidation mediataed cell injury. *Pathophysiology* **2017**, *24*, 39–44.
18. Chattopadhyay, P.; Shukla, G.; Wahi, A.K. Folic acid inhibits necrosis and apoptosis in ischemic and reperfusion induced injury in rat liver. *Orient. Pharm. Exp. Med.* **2009**, *9*, 67–73. [[CrossRef](#)]
19. Carson, L.; Kelly-Brown, C.; Stewart, M.; Oki, A.; Regisford, G.; Luo, Z.P.; Bakmutov, V.I. Synthesis and characterization of chitosan-carbon nanotube composites. *Mater. Lett.* **2009**, *63*, 617–620. [[CrossRef](#)]
20. Ghosh, G.; Naskar, M.K.; Patra, A.; Chatterjee, M. Synthesis and characterization of PVP-encapsulated ZnS nanoparticles. *Opt. Mater.* **2006**, *28*, 1047–1053. [[CrossRef](#)]
21. Hsu, S.-C.; Don, T.-M.; Chiu, W.-Y. Free radical degradation of chitosan with potassium persulfate. *Polym. Degrad. Stabil.* **2002**, *75*, 73–83. [[CrossRef](#)]
22. Mihara, M.; Uchiyama, M. Determination of malonaldehyde precursor in tissues by thiobarbituric acid test. *Anal. Biochem.* **1978**, *86*, 271–278.
23. Ellman, G.L. Tissue sulfhydryl groups. *Arch. Biochem. Biophys.* **1959**, *82*, 70–77. [[CrossRef](#)]
24. Sinha, A.K. Colorimetric assay of catalase. *Anal. Biochem.* **1972**, *47*, 389–394. [[CrossRef](#)]
25. Bancroft, J.D.; Gamble, M. *Theory and Practice of Histological Techniques*; Elsevier Health Sciences: Amsterdam, The Netherlands; Churchill Livingstone: London, UK, 2008.
26. Xiao, Y.B.; Lin, Z.T.; Chen, Y.M.; Wang, H.; Deng, Y.L.; Le, D.E.; Bin, J.G.; Li, M.Y.; Liao, Y.L.; Liu, Y.L.; et al. High molecular weight chitosan derivative polymeric micelles encapsulating superparamagnetic iron oxide for tumor-targeted magnetic resonance imaging. *Int. J. Nanomed.* **2015**, *10*, 1155–1172.
27. Bujňáková, Z.; Dutková, E.; Zorkovská, A.; Baláž, M.; Kováč, J.; Kello, M.; Mojžiš, J.; Briančin, J.; Baláž, P. Mechanochemical synthesis and in vitro studies of chitosan-coated InAs/ZnS mixed nanocrystals. *J. Mater. Sci.* **2017**, *52*, 721–735. [[CrossRef](#)]
28. Liu, J.; Guo, T.F.; Shi, Y.J.; Yang, Y. Solvation induced morphological effects on the polymer/metal contacts. *J. Appl. Phys.* **2001**, *89*, 3668–3673. [[CrossRef](#)]
29. Ryu, S.R.; Noda, I.; Jung, Y.M. What is the origin of positional fluctuation of spectral features: True frequency shift or relative intensity changes of two overlapped bands? *Appl. Spectrosc.* **2010**, *64*, 1017–1021. [[CrossRef](#)] [[PubMed](#)]
30. Pujana, M.A.; Perez-Alvarez, L.; Iturbe, L.C.; Katime, I. pH-sensitive chitosan-folate nanogels crosslinked with biocompatible dicarboxylic acids. *Eur. Polym. J.* **2014**, *61*, 215–225. [[CrossRef](#)]
31. Ribeiro, M.V.M.; Melo, I.S.; Lopes, F.C.C.; Moita, G.C. Development and validation of a method for the determination of folic acid in different pharmaceutical formulations using derivative spectrophotometry. *J. Pharm. Sci.* **2016**, *52*, 741–750. [[CrossRef](#)]
32. Mende, M.; Schwarz, D.; Steinbach, C.; Boldt, R.; Schwarz, S. Simultaneous adsorption of heavy metal ions and anions from aqueous solutions on chitosan Investigated by spectrophotometry and SEM-EDX analysis. *Colloid. Surface. Physicochem. Eng. Aspect.* **2016**, *510*, 275–282. [[CrossRef](#)]
33. Babior, B.M. The respiratory burst oxidase. *Adv. Enzymol. Relat. Areas Mol. Biol.* **1992**, *65*, 49–65.
34. Mates, J.M.; Gomez, C.P.; Nunez, C. Antioxidant enzymes and human diseases. *Clin. Biochem.* **1999**, *32*, 595–603. [[CrossRef](#)]
35. Gul, M.; Kutay, F.Z.; Temocin, S.; Hanninen, O. Cellular and clinical implication of glutathione. *Indian J. Exp. Biol.* **2000**, *38*, 625–634. [[PubMed](#)]
36. Chandrasekara, N.; Shahidi, F. Antioxidative potential of cashew phenolics in food and biological model systems as affected by roasting. *Food Chem.* **2011**, *129*, 1388–1396. [[CrossRef](#)]
37. De Boer, V.C.J.; Dihal, A.A.; van der Woude, H.; Arts, I.C.W.; Wolfram, S.; Alink, G.M.; Rietjens, I.M.C.M.; Keijer, J.; Hollman, P.C.H. Tissue distribution of quercetin in rats and pigs. *J. Nutr.* **2005**, *135*, 1718–1725. [[CrossRef](#)]
38. Slater, T.F. Free radicals in medicine. *Free. Radic. Res. Commun.* **1989**, *7*, 119–130.
39. Kokilavani, V.; Devi, M.A.; Sivarajan, K.; Panneerselvam, C. Combined efficacies of DL-lipoic acid and meso 2, 3dimercaptosuccinic acid against arsenic induced toxicity in antioxidant systems of rats. *Toxicol. Lett.* **2005**, *160*, 1–7. [[CrossRef](#)]

40. Sinha, M.; Manna, P.; Sil, P.C. Terminalia arjuna protects mouse hearts against sodium fluoride-induced oxidative stress. *J. Med. Food* **2008**, *11*, 733–740. [[CrossRef](#)]
41. Kirkman, M.N.; Gaetani, G.F. Catalase: A tetrameric enzyme with four tightly bound molecules of NADPH. *Proc. Natl. Acad. Sci. USA* **1984**, *81*, 4343–4347. [[CrossRef](#)]
42. Shanthakumari, D.; Srinivasalu, S.; Subramanian, S. Effect of fluoride intoxication on lipid peroxidation and antioxidant status in experimental rats. *Toxicology* **2004**, *204*, 219–228. [[CrossRef](#)]
43. Cos, P.; Ying, L.; Calomme, M.; Hu, J.P.; Cimanga, K.; Poel, B.V.; Pieters, L.; Vlietinck, A.J.; Berghe, D.V. Structure-activity relationship and classification of flavonoids as inhibitors of xanthine oxidase and superoxide scavengers. *J. Nat. Prod.* **1998**, *61*, 71–76. [[CrossRef](#)] [[PubMed](#)]
44. Mira, L.; Silva, M.; Rocha, R.; Manso, C.F. Measurement of relative antioxidant activity of compounds: A methodological note. *Redox Rep.* **1999**, *4*, 69–74. [[CrossRef](#)]
45. Morel, I.; Lescoat, G.; Cogrel, P.; Sergent, O.; Padeloup, N.; Brissot, P.; Cillard, J. Antioxidant and iron-chelating activities of the flavonoids catechin, quercetin and diosmetin on iron-loaded rat hepatocyte cultures. *Biochem. Pharmacol.* **1993**, *45*, 13–19. [[CrossRef](#)]
46. Tzankova, V.; Aluani, D.; Kondeva-Burdina, M.; Yordanov, Y.; Odzhakov, F.; Apostolov, A.; Yoncheva, K. Hepatoprotective and antioxidant activity of quercetin loaded chitosan/alginate particles in vitro and in vivo in a model of paracetamol-induced toxicity. *Biomed. Pharmacother.* **2017**, *92*, 569–579. [[CrossRef](#)] [[PubMed](#)]
47. Hamza, R.Z.; Gobouri, A.A.; Al-Yasi, H.M.; Al-Talhi, T.A.; El-Megharbel, S.M. A new sterilization strategy using TiO₂ nanotubes for production of free radicals that eliminate viruses and application of a treatment strategy to combat infections caused by emerging SARS-CoV-2 during the COVID-19 pandemic. *Coatings* **2021**, *11*, 680. [[CrossRef](#)]
48. El-Wahed, M.G.A.; Refat, M.S.; El-Megharbel, S.M. Synthesis, spectroscopic and thermal characterization of some transition metal complexes of folic acid. *Spectrochim. Acta Part A Mol. Biomol. Spectrosc.* **2008**, *70*, 916–922. [[CrossRef](#)]
49. Refat, M.S.; Hamza, R.Z.; A Adam, A.M.; Saad, H.A.; Gobouri, A.A.; Azab, E.; Al-Salmi, F.A.; Altalhi, T.A.; Khojah, E.; Gaber, A.; et al. Antioxidant, antigenotoxic, and hepatic ameliorative effects of quercetin/zinc complex on cadmium-induced hepatotoxicity and alterations in hepatic tissue structure. *Coatings* **2021**, *11*, 501. [[CrossRef](#)]
50. Refat, M.S.; Hamza, R.Z.; Adam, A.M.A.; Saad, H.A.; Gobouri, A.A.; Al-Harbi, F.S.; Al-Salmi, F.A.; Altalhi, T.; El-Megharbel, S.M. Quercetin/Zinc complex and stem cells: A new drug therapy to ameliorate glycometabolic control and pulmonary dysfunction in diabetes mellitus: Structural characterization and genetic studies. *PLoS ONE* **2021**, *16*, e0246265. [[CrossRef](#)]
51. Nabavi, S.M.; Nabavi, S.F.; Eslami, S.; Moghaddam, A.H. In vivo protective effects of quercetin against sodium fluoride-induced oxidative stress in the hepatic tissue. *Food Chem.* **2012**, *132*, 931–935. [[CrossRef](#)]
52. Hamza, R.Z.; Al-Salmi, F.A.; El-Shenawy, N.S. Chitosan and lecithin ameliorate osteoarthritis symptoms induced by monoiodoacetate in a rat model. *Molecules* **2020**, *25*, 5738. [[CrossRef](#)]